Phase diagram of chiral and diquark condensates
at finite temperature and density
in the 2-dimensional Gross Neveu model

Hiroaki Kohyama[*]

Department of Physics, Osaka City University,

Sumiyoshi-ku, Osaka 558-8585, JAPAN

(Dated: April 30, 2008)

Abstract

We construct the phase diagram of the chiral and diquark condensates at finite temperature and density in the $1+1$ dimensional (2D) two flavor massless Gross Neveu model. The resultant phase diagram shows (I) the chiral condensed phase at low temperature and density, (II) the diquark condensed phase at low temperature and high density, and (III) the chiral and diquark coexisting phase at low temperature and intermediate density. This phase structure is also seen in the 3D Gross Neveu model and the 4D Nambu Jona-Lasinio (NJL) model. Thus the phase diagrams of the chiral and diquark condensates in the NJL-type models do not change qualitatively in 2D, 3D and 4D.

PACS numbers: 12.38.Aw, 12.38.Lg, 11.15.Pg, 11.10.Wx

[*]Electronic address: kohyama@sci.osaka-cu.ac.jp

I. INTRODUCTION

Studying the phase structure of Quantum Chromodynamics (QCD) is one of the most interesting topics in the field of strong interaction physics. QCD is an asymptotically free theory [1], and the interaction between quarks and gluons becomes weak at high temperature and density. Then the quarks can be free particles at high temperature and density, and this system is called the quark-gluon-plasma. On the other hand, at low temperature and density, quarks are confined into hadrons and can not be observed as free particles. Furthermore, it is widely believed that the color superconducting phases are realized at low temperature and high baryon density. The color superconductivity is the state where the quark-quark (diquark) Cooper pairs [2] become correlated, which condense. Since it was indicated that color superconducting phases have non-negligible region in the QCD phase diagram[3], there has been a lot of works on it. For review articles, see [4]. Color superconductivity is important because it might be observed in compact stars, such as neutron stars. The density of a neutron star is about ten times of that of the normal nuclear. This density corresponds to a quark chemical potential $\mu \sim 500\text{MeV}$ where the deconfinement phase transition may happen. Thus it is physically reasonable to expect that color superconducting states are realized in neutron stars.

Investigation of these subjects from QCD is still a challenge to theorists, and we usually have to rely on some effective theories of QCD. One of the most important models is the Nambu Jona-Lasinio (NJL) model [5] which is a low energy effective theory of QCD. Since the NJL model successfully describes the phenomena of the transition from chiral broken phase to chiral restored phase, a variety of works has been devoted to the study based on it [6]. Recently, it was found that the NJL model also describes the phase transition from chiral broken phase to color superconducting phase [7], and the phase diagram of the NJL model shows similar structure with the QCD phase diagram. Thus the NJL model is also effective when we consider a color superconductivity.

The study of the phase structure of the NJL model in lower dimensions (D) is also an interesting issue, because the model usually becomes simpler in lower dimensions [8]. Indeed, the NJL model is renormalizable in 2D and 3D. The NJL-type model in lower dimensions is the Gross Neveu (GN) model, which is proposed in 1974 [9]. The GN model shares many properties with QCD, such as asymptotic freedom and chiral symmetry breaking in vacuum,

and there has been a lot of works on it [10, 11, 12, 13, 14, 15]. The phase diagram of quark-antiquark condensate in the 2D and 3D GN model was obtained in [12] and [13]. By using the mean-field approximations, the phase structure of the quark-antiquark ($q\bar{q}$) and diquark (qq) condensates in the 3D GN model with 4-component spinor quarks was derived in [14]. Although the possibility of spontaneously symmetry breaking is excluded by the Mermin-Wagner-Coleman theorem, however, I believe that the study of the $q\bar{q}$ and qq condensates near the Fermi surface is important from the phenomenological point of view. Actually, it was shown that the $q\bar{q}$ and qq condensates could be formed in the 3D GN model by using the effective potential analysis [14]. The resultant phase diagrams show considerably similar structure to the case of the 4D NJL model. This may suggest that the phase structure of the quark matter does not change qualitatively in the cases of lower dimensions. To confirm this idea, we focus on the phase structure in the 2D GN model here. Recently, within the 2D GN model, the $q\bar{q}$ and qq condensates in vacuum (zero temperature and chemical potential) has been studied in [15], and it has been found that the competition between these condensates is sensitive to the ratio of the coupling strengths of the $q\bar{q}$ and qq condensates.

In this paper, we study the $q\bar{q}$ and qq condensates at finite temperature and density in the 2D two flavor massless GN model, and obtain the phase diagrams. Then we compare the result with those of the 3D GN model and the 4D NJL model.

The paper is constituted as follows: In Sec.II, we introduce the Lagrangian density of the 2D GN model and apply the mean-field approximation. In Sec.III, the thermodynamic potential is obtained. Then we display the numerical results for the $q\bar{q}$ and qq condensates at zero and finite temperatures in Sec.IV. The phase diagrams of the 2D GN model are shown in Sec.V. Finally in Sec.VI, we compare the results of the 2D, 3D GN models and 4D NJL model, and discuss the similarities and differences of them.

II.   2D GROSS NEVEU MODEL

A.   Preliminary

We consider the following Lagrangian density as the original form of the four fermion interaction model,

$$\mathcal{L} = \bar{q}i\partial\!\!\!/q + G_S(\bar{q}q)^2. \tag{1}$$

3

Here G_S is the coupling constant of the $q\bar{q}$ condensate. To incorporate the diquark condensate in this Lagrangian, we apply the Fiertz transformation to $(q\bar{q})^2$ term and leave the most relevant interaction near the Fermi surface [3]. More concretely, the diquark interacting term is determined as follows: Let us write the diquark term as $(q^{\mathrm{T}}\mathcal{O}q)^2$ in its most general form, where $\mathcal{O}$ is an operator in spinor, flavor and color spaces. The Pauli principle,

$$q^{\mathrm{T}}\mathcal{O}q = \mathcal{O}_{ij}q_i q_j = -\mathcal{O}_{ij}q_j q_i = -q^{\mathrm{T}}\mathcal{O}^{\mathrm{T}}q, \tag{2}$$

indicates that $\mathcal{O}$ is a totally antisymmetric operator. Since the attractive interaction becomes the dominant contribution near the Fermi surface [3], we select the color antitriplet matrices $(\lambda_2, \lambda_5, \lambda_7)$ in color space. The renormalization group arguments [16] force the operator in spinor space to be antisymmetric. Then the operator in flavor space has to be antisymmetric. Observing the above mentioned consideration, we choose the Lagrangian density of the form

$$\mathcal{L} = \bar{q}i\slashed{\partial}q + G_S(\bar{q}q)^2 + G_D \sum_{a=2,5,7}(\bar{q}i\tau_2\lambda_a\gamma^5 q^C)(\bar{q}^C i\tau_2\lambda_a\gamma^5 q), \tag{3}$$

where τ_2 is the second Pauli matrix in flavor space and C in q^C expresses the charge conjugation. The charge conjugated fields are given by $q^C = C\bar{q}^{\mathrm{T}}$, $\bar{q}^C = q^{\mathrm{T}}C$, with the charge conjugation matrix C. Since a vector in color space can be rotated into one direction by a global $SU(3)$-color transformation, one can select a color direction to *blue* without loss of generality. This is equivalent to leave λ_2 in Eq.(3), and we have the diquark term $(\bar{q}i\tau_2\lambda_2\gamma^5 q^C)(\bar{q}^C i\tau_2\lambda_2\gamma^5 q)$.

B.   The model

Following the reason discussed in the previous subsection, we employ the Lagrangian density for the 2D two flavor massless GN model with the diquark condensate term,

$$\mathcal{L} = \bar{q}i\slashed{\partial}q + G_S(\bar{q}q)^2 + G_D(\bar{q}i\tau_2\lambda_2\gamma^5 q^C)(\bar{q}^C i\tau_2\lambda_2\gamma^5 q). \tag{4}$$

In 2D, $q \equiv q_{\alpha k}(t,x)$ is two component spinor fields with the two flavors $\alpha = u, d$ and three colors $k = r$ (red), g (green), b (blue). For γ matrix, we use the following representation,

$$\gamma^0 = \begin{pmatrix} 1 & 0 \\ 0 & -1 \end{pmatrix}, \gamma^1 = \begin{pmatrix} 0 & 1 \\ -1 & 0 \end{pmatrix} = -C, \quad \gamma^5 = \gamma^0\gamma^1. \tag{5}$$

The Lagrangian Eq.(4) is invariant under the following transformations:

1. Parity $\mathcal{P}$: $q(t,x) \to \gamma^0 q(t,-x)$

2. Time reversal $\mathcal{T}$: $q(t,x) \to \gamma^0 q(-t,x)$

3. Charge conjugation $\mathcal{C}$: $q^C \to -\gamma^1 \bar{q}^{\mathrm{T}}, \quad \bar{q}^C \to -q^{\mathrm{T}}\gamma^1$

4. Discrete chiral symmetry $\mathcal{X}_D$: $q \to \gamma^5 q$.

The symmetry properties are discussed in the paper [15] in more detail.

Within the mean-field approximation, the Lagrangian density turns out to be

$$\tilde{\mathcal{L}} = \bar{q}i\slashed{\partial}q - \bar{q}\sigma q + \frac{1}{2}\Delta^*(\bar{q}^C i\tau_2\lambda_2\gamma^5 q) + \frac{1}{2}\Delta(\bar{q}i\tau_2\lambda_2\gamma^5 q^C) - \frac{\sigma^2}{4G_S} - \frac{|\Delta|^2}{4G_D}. \tag{6}$$

Here σ and Δ are the order parameters for the chiral and diquark condensates,

$$\sigma = -2G_S\langle\bar{q}q\rangle \quad \text{and} \quad \Delta = 2G_D\langle\bar{q}^C i\tau_2\lambda_2\gamma^5 q\rangle. \tag{7}$$

III.   THE THERMODYNAMIC POTENTIAL

A.   Derivation of the thermodynamic potential

The partition function is evaluated by using the standard procedure,

$$\mathcal{Z} = N' \int [d\bar{q}][dq]\exp\left\{\int_0^\beta d\tau \int dx\left(\tilde{\mathcal{L}} + \mu\bar{q}\gamma_0 q\right)\right\}, \tag{8}$$

where $\beta = 1/T$ is the inverse temperature and μ is the quark chemical potential. Introduction of the Nambu-Gorkov basis [17]

$$\Psi = \begin{pmatrix} q \\ q^C \end{pmatrix} \quad \text{and} \quad \bar{\Psi} = \begin{pmatrix} \bar{q} & \bar{q}^C \end{pmatrix}, \tag{9}$$

enables us to write the partition function in the simple form,

$$\begin{aligned}
\mathcal{Z} = &N'\exp\left\{-\int_0^\beta d\tau \int dx\left(\frac{\sigma^2}{4G_S} + \frac{|\Delta|^2}{4G_D}\right)\right\} \\
&\times \int [d\Psi]\exp\left\{\frac{1}{2}\sum_{n,p}\bar{\Psi}\left(\beta G^{-1}\right)\Psi\right\}.
\end{aligned} \tag{10}$$

The matrix G^{-1} is defined by

$$G^{-1} = \begin{pmatrix} (\slashed{p} - \sigma + \mu\gamma^0)\mathbf{1}_f\mathbf{1}_c & i\tau_2\lambda_2\gamma^5\Delta \\ i\tau_2\lambda_2\gamma^5\Delta^* & (\slashed{p} - \sigma - \mu\gamma^0)\mathbf{1}_f\mathbf{1}_c \end{pmatrix}, \tag{11}$$

5

where $\mathbf{1}_f$ and $\mathbf{1}_c$ are the unit matrices in flavor and color spaces, respectively.

Then the thermodynamic potential $\Omega = -\ln \mathcal{Z}/\beta V$ becomes

$$\Omega(\sigma, |\Delta|) = \frac{\sigma^2}{4G_S} + \frac{|\Delta|^2}{4G_D} - \frac{1}{\beta V} \ln \int [d\Psi] \exp\left[\frac{1}{2}\sum_{n,p} \bar{\Psi}(\beta G^{-1})\Psi\right], \tag{12}$$

where V is the volume of the thermal system. With the help of the formula

$$\int [d\Psi] \exp\left[\frac{1}{2}\sum_{n,p} \bar{\Psi}(\beta G^{-1})\Psi\right] = \det^{1/2}(\beta G^{-1}), \tag{13}$$

we have

$$\Omega(\sigma, |\Delta|) = \frac{\sigma^2}{4G_S} + \frac{|\Delta|^2}{4G_D} - \frac{1}{\beta V} \ln \det^{1/2}(\beta G^{-1}). \tag{14}$$

The determinant is calculated by following the same procedure in [7],

$$\det^{1/2}(G^{-1}) = \left[p_0^2 - E_\Delta^{+2}\right]^2 \left[p_0^2 - E_\Delta^{-2}\right]^2 \left[p_0^2 - E^{+2}\right] \left[p_0^2 - E^{-2}\right], \tag{15}$$

where $p_0 = i(2n+1)\pi T$, $(n = \cdots, -2, -1, 0, 1, 2, \cdots)$ and

$$E_\Delta^{\pm 2} \equiv (E \pm \mu)^2 + |\Delta|^2, \ E^\pm \equiv E \pm \mu, E \equiv \sqrt{p_1^2 + \sigma^2}. \tag{16}$$

Then, we obtain

$$\Omega(\sigma, |\Delta|) = \frac{\sigma^2}{4G_S} + \frac{|\Delta|^2}{4G_D}$$
$$- 2T\sum_\pm \sum_n \int \frac{dp_1}{2\pi}\left[\ln[\beta^2(p_0^2 - E^{\pm 2})] + 2\ln[\beta^2(p_0^2 - E_\Delta^{\pm 2})]\right]. \tag{17}$$

The frequency summation is performed through using the standard method [18],

$$\sum_n \ln[\beta^2(p_0^2 - E^2)] = \beta[E + 2T\ln(1 + e^{-\beta E})]. \tag{18}$$

Thus we finally arrive at

$$\Omega(\sigma, |\Delta|) = \Omega_0(\sigma, |\Delta|) + \Omega_T(\sigma, |\Delta|), \tag{19}$$

$$\Omega_0(\sigma, |\Delta|) = \frac{\sigma^2}{4G_S} + \frac{|\Delta|^2}{4G_D} - 2\int \frac{dp_1}{2\pi}[E + E_\Delta^+ + E_\Delta^-], \tag{20}$$

$$\Omega_T(\sigma, |\Delta|) = -2T\sum_\pm \int \frac{dp_1}{2\pi}\left[\ln(1 + e^{-\beta E^\pm}) + 2\ln(1 + e^{-\beta E_\Delta^\pm})\right]. \tag{21}$$

Ω_0 is T independent contribution, which is ultraviolet divergent, while T dependent part Ω_T is finite. For the purpose of later use, we rewrite Ω_0 in the integral form in the 2D Euclidean momentum space,

$$\Omega_0(\sigma, |\Delta|) = \frac{\sigma^2}{4G_S} + \frac{|\Delta|^2}{4G_D} - \sum_{\pm} \int \frac{d^2 p_E}{(2\pi)^2} \left[\ln\left(\frac{p_{E0}^2 + E^{\pm 2}}{p_E^2} \right) + 2\ln\left(\frac{p_{E0}^2 + E_{\Delta}^{\pm 2}}{p_E^2} \right) \right]. \quad (22)$$

The p_E^2 terms in the denominators in the arguments of logarithms are inserted so as to drop an irrelevant infinite constant.

B. Renormalized thermodynamic potential

To eliminate the divergence, we perform the renormalization by introducing the counter Lagrangian density[14], $\mathcal{L}_C = -Z_S \sigma^2/2 - Z_D |\Delta|^2$. The renormalization factors Z_S and Z_D become

$$Z_S = \frac{6}{\pi \epsilon} + \frac{6}{\pi} \ln \alpha^2,$$
$$Z_D = \frac{2}{\pi \epsilon} + \frac{2}{\pi} \ln \alpha^2, \quad (23)$$

where $\epsilon \, (\equiv 2 - D)$ is the dimensional regularization parameter and α is an arbitrary renormalization scale.

Let us introduce the following parameters

$$\sigma_0 \equiv |\alpha| e^{-\pi/(12 G_S)}, \quad (24)$$

$$\Delta_0 \equiv |\alpha| e^{-\pi/(8 G_D)}, \quad (25)$$

where $\sigma_0 \, (\Delta_0)$ is the $q\bar{q} \, (qq)$ condensate at $T = 0 = \mu$ in the model in which the $qq \, (q\bar{q})$ condensate is absent. By using the above parameters, we finally obtain the renormalized thermodynamic potential:

$$\Omega_r(\sigma, |\Delta|) = \Omega_{0r}(\sigma, |\Delta|) + \Omega_T(\sigma, |\Delta|), \quad (26)$$

$$\Omega_{0r}(\sigma, |\Delta|) = -\left(\frac{3\pi}{2} \ln \sigma_0^2 \right) \sigma^2 - \left(\pi \ln \Delta_0^2 \right) |\Delta|^2$$
$$- \sum_{\pm} \int \frac{d^2 p_E}{(2\pi)^2} \left[\ln\left(\frac{p_{E0}^2 + E^{\pm 2}}{p_E^2} \right) + 2\ln\left(\frac{p_{E0}^2 + E_{\Delta}^{\pm 2}}{p_E^2} \right) - \frac{3}{p_E^2} \sigma^2 - \frac{2}{p_E^2} |\Delta|^2 \right]. \quad (27)$$

Note that the thermodynamic potential Ω_r has two free parameters (σ_0, Δ_0). As in [14], we take σ_0 to be the scale of the theory ($\sigma_0 \geq 0$), and choose the ratio Δ_0/σ_0 as a parameter.
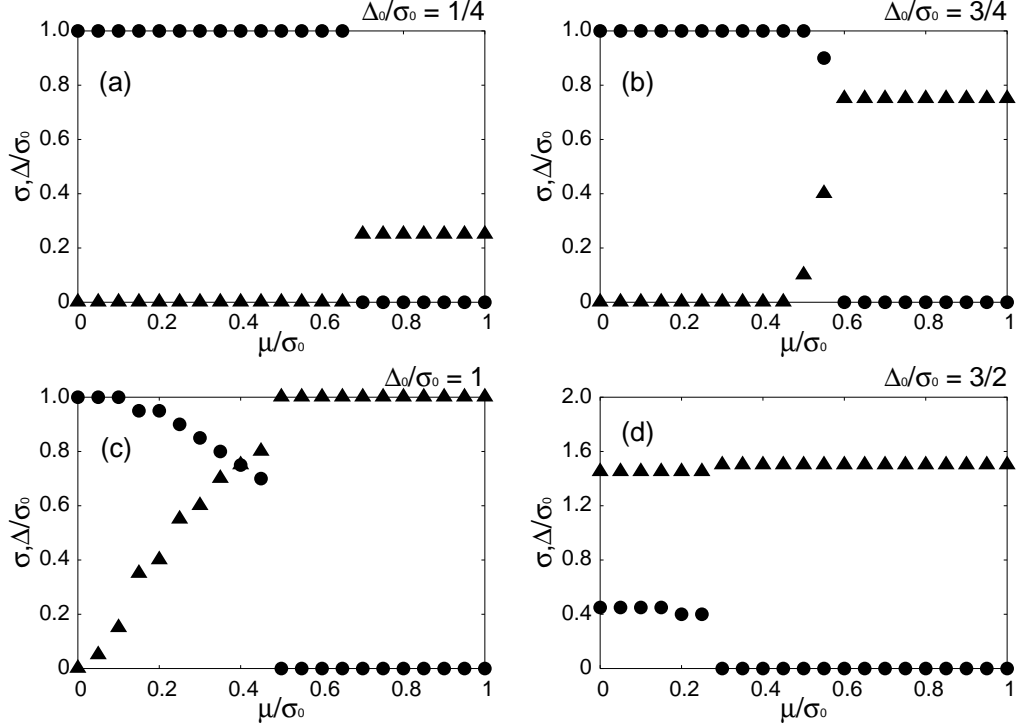
FIG. 1: The chiral(circles) and diquark(triangles) condensates at $T = 0$.

IV. THE CHIRAL AND DIQUARK CONDENSATES

In this section, we show the numerical results for the chiral and diquark condensates at zero and finite temperatures. Through minimizing the thermodynamic potential, we study the $q\bar{q}$ and qq condensates.

In Fig. 1, we display the results for the $q\bar{q}$ and qq condensates at $T = 0$. For $\Delta_0/\sigma_0 = 1/4$ (panel (a)), we see that the $q\bar{q}$ condensate is realized for $\mu = 0 \sim 0.65\sigma_0$ and there dose not arise the qq condensate. At $\mu = 0.7\sigma_0$, the $q\bar{q}$ condensate disappears and the qq condensate occurs, which indicates the phase transition from $q\bar{q}$ condensed phase to the qq condensed phase. Similar results are obtained for $\Delta_0/\sigma_0 = 3/4$, 1 where the $q\bar{q}$ condensate is dominant at low μ and the qq condensate dominates at high μ. However in the panel (d) ($\Delta_0/\sigma_0 = 3/2$), the qq condensate is dominant for whole μ, and the $q\bar{q}$ condensate is small compare to the qq condensate. Thus the behaviors of the $q\bar{q}$ and qq condensates are sensitive to the value of the ratio Δ_0/σ_0.

In Fig. 2, we plot the results at finite temperature for $\Delta_0/\sigma_0 = 1/4$, 1 and $\mu = 0$, $0.4\sigma_0$. For $(\Delta_0/\sigma_0, \mu) = (1/4, 0)$, the $q\bar{q}$ condensate starts to decrease at $T = 0.25\sigma_0$ and completely
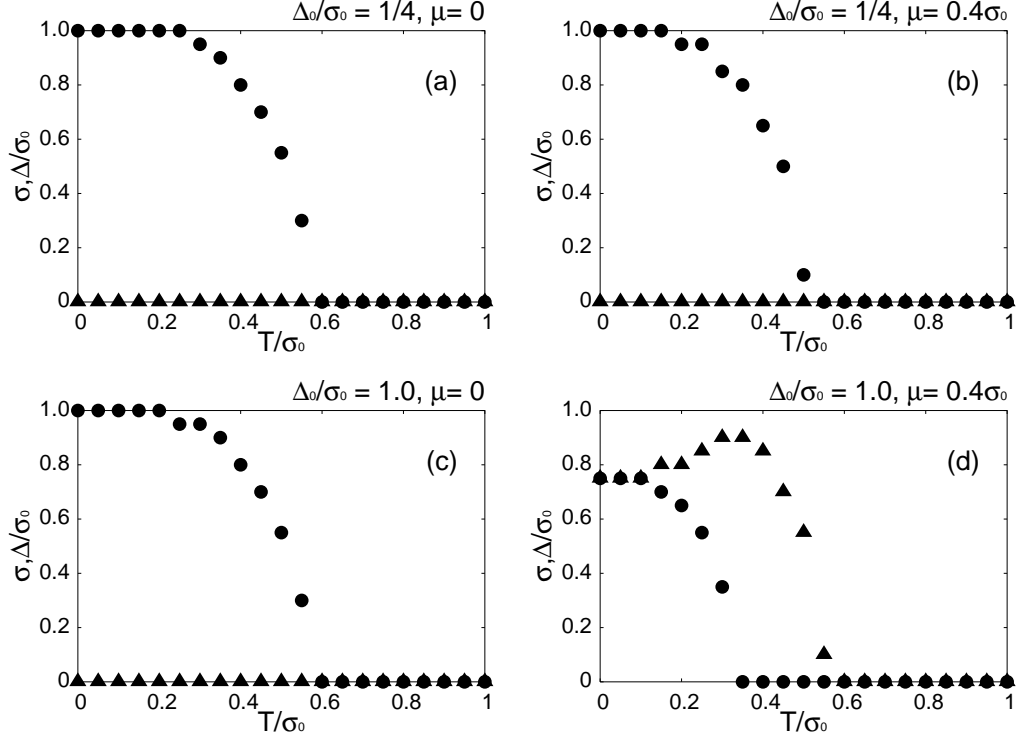
FIG. 2: The $q\bar{q}$(circles) and qq(triangles) condensates at finite temperature.

disappears at $T = 0.6\sigma_0$. For the cases $(\Delta_0/\sigma_0, \mu) = (1/4, 0.4\sigma_0)$ and $(1, 0)$, we observe the similar behavior: The $q\bar{q}$ condensate decreases when T increases and the qq condensate does not arise. In the panel (d) $(\Delta_0/\sigma_0, \mu) = (1, 0.4\sigma_0)$, the qq condensate exists and it decreases with increasing temperature. Thus, the $q\bar{q}$ and qq condensates decrease when T becomes larger, which is the reasonable result because the theory is asymptotically free. We have carried out the numerical calculation for the other values of Δ_0/σ_0, and found that the behaviors do not alter qualitatively.

It is to be noted that the $q\bar{q}$ condensate reduces to zero discontinuously at $T = 0$ (see Fig. 1). While it decreases continuously at finite temperature for some parameter region. These are the signals of the first order and second order phase transitions. The above mentioned results indicate that the critical point from first order phase transition to second order one appears in the phase diagram, which we will discuss in more detail in the next section.
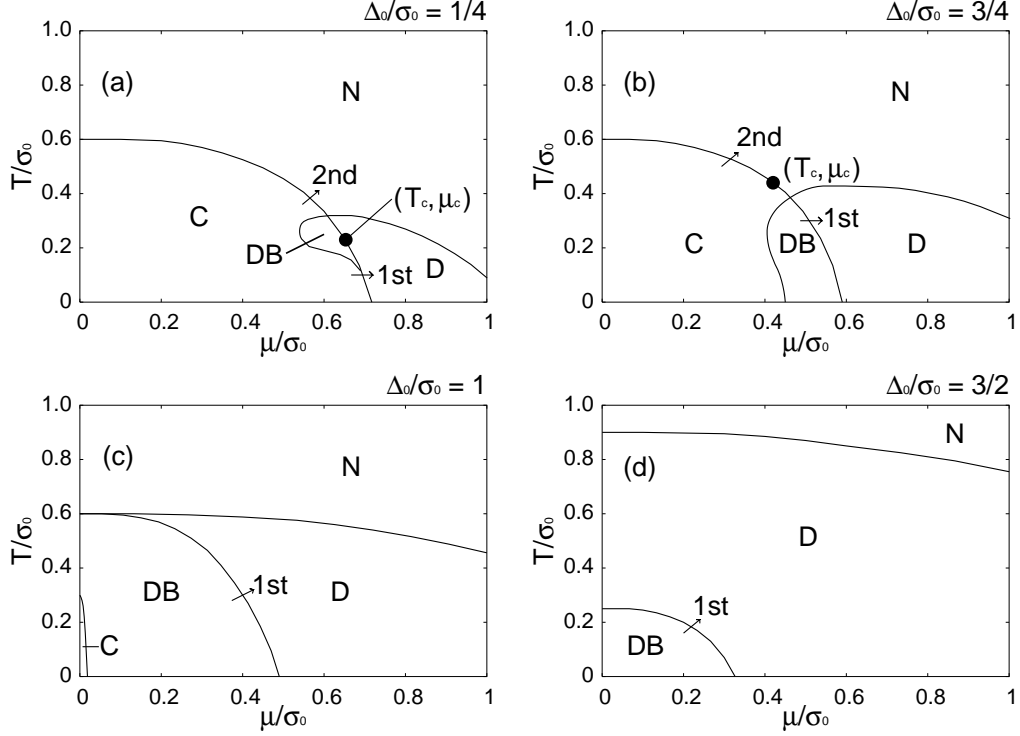
FIG. 3: The phase diagrams.

V.   THE PHASE DIAGRAM

Fig. 3 displays the phase diagrams for the cases $\Delta_0/\sigma_0 = 1/4$, 3/4, 1, 3/2. As seen in the diagrams, there appear the following phases:

C: Chiral condensed phase ($\sigma \neq 0$, $\Delta = 0$)

D: Diquark condensed phase($\sigma = 0$, $\Delta \neq 0$)

DB: Double Broken phase ($\sigma \neq 0$, $\Delta \neq 0$)

N: Normal phase ($\sigma = 0$, $\Delta = 0$)

For small Δ_0/σ_0, the C phase is realized at low T and μ, the DB phase occurs at low T and intermediate μ and the D phase at low T and high μ. This phase structure bears resemblance to the QCD phase diagram. However, when Δ_0/σ_0 is large, the C phase no longer appears and the DB phase exists at low T and μ, and the D phase does at low T and high μ. Thus, as the ratio Δ_0/σ_0 increases, the region of the C phase becomes smaller and those of the DB phase and D phase enlarge.

The black circles (T_c, μ_c) seen in Fig. 3(a) and (b) are the critical points from the first order phase transition to the second order one. When $T < T_c$, the transition is of the first order and it is of the second order for $T > T_c$. From the figure, we find that the critical point moves along the transition line toward $\mu = 0$ as the ratio Δ_0/σ_0 increases. The critical point no longer appears at $\Delta_0/\sigma_0 = 1$, and the transition from the DB phase to D phase is of the first order. The other phase transitions, D $\rightarrow$ N and C $\rightarrow$ DB, are always of the second order.

VI.   CONCLUDING REMARKS

Through studying the $q\bar{q}$ and qq condensates at finite temperature and density, we have obtained phase diagrams. When the ratio Δ_0/σ_0 is small, there appears the chiral condensed (C) phase at low T and μ, the diquark condensed (D) phase at low T and high μ, and the double broken (DB) phase at low T and intermediate μ. On the other hand, for large Δ_0/σ_0, the DB phase is realized at low T and μ and the D phase at low T and high μ. Thus the phase structure drastically changes with respect to the ratio Δ_0/σ_0. Such a behavior of the phase diagrams shows close similarity with the ones in the 3D GN model.

The direct comparison of the present model and the 4D NJL model is difficult since the free parameter of these models are different. In the 4D NJL model, the parameter is the ratio of two coupling constants G_D/G_S[7], and, in the present model, the parameter is the ratio Δ_0/σ_0. However Δ_0 is related to G_D through Eq.(25), and it increases as G_D increases. This means that Δ_0/σ_0 increases as G_D becomes larger. Then, with increasing G_D, the phase diagram changes from Fig. 3(a) to (d). After all this, we see that the phase structure bears resemblance to the 4D NJL case.

Having compared the 2D GN model, 3D GN model and 4D NJL model, we see that the similar phase structure is realized in all models. This indicates that the phase structure of $q\bar{q}$ and qq condensates in the NJL-type model does not change appreciably in 2D, 3D and 4D.

---

[1] D. J. Gross and F. Wilczek, Phys. Rev. Lett. **30** (1973) 1343; H. D. Politzer, *ibid.* **30** (1973) 1346.

[2] L. N. Cooper, Phys. Rev. **104** (1956) 1189.

[3] M. Alford, K. Rajagopal, F. Wilczek, Phys. Lett. B **422** (1998) 247.

[4] K. Rajagopal, F. Wilczek, hep-ph/0011333; D. K. Hong, Acta Phys. Polon. B **32**, (2001) 1253; M. G. Alford, Ann. Rev. Nucl. Part. Sci. **51**, (2001) 131; G. Nardulli, Riv. Nuovo Cim. **25N3**, 1 (2002); T. Schafer, arXiv:hep-ph/0304281. D. H. Rischke, Prog. Part. Nucl. Phys. **52** (2004) 197;

[5] Y. Nambu and G. Jona-Lasinio, Phys. Rev. **122** (1961) 345; *ibid.* **124** (1961) 246.

[6] T. Hatsuda and T. Kunihiro, Phys. Rept. **247** (1994) 221; M. Buballa, Phys. Rept. **407** (2005) 205.

[7] M. Huang, Int. J. Mod. Phys. E**14** (2005) 675.

[8] S. Weinberg, Phys. Rev. D**56** (1997) 2303.

[9] D. J. Gross and A. Neveu, Phys. Rev. D**10** (1974) 3235.

[10] B. Rosenstein, B. J. Warr, S. H. Park, Phys. Rep. **205** (1991) 59.

[11] T. Inagaki, T. Kouno and T. Muta, Int. J. Mod. Phys. A **10** (1995) 2241; S. Kanemura, H.-T. Sato, Mod. Phys. Lett. A**10** (1995) 1777; D. Ebert, K. G. Klimenko, H. Toki, Phys. Rev. D**64** (2001) 014038; A. P. C. Malbouisson, J. M. C. Malbouisson, A. E. Santana, J. C. da Silva, Int. J. Mod. Phys. A**20** (2005) 4638; J. Feinberg, S. Hillel, J. Phys. A**39** (2006) 6341; J.-L. Kneur, M. B. Pinto, R. O. Ramos, Phys. Rev. D**74** (2006) 125020; B. Charneski, A. F. Ferrari, M. Gomes, J. Phys. A**40** (2007) 3633; H. Kohyama, Phys. Rev. D**77** (2008) 045016; A. Niegawa, arXiv:0801.1937.

[12] U. Wolff, Phys. Lett. B**157** (1985) 303.

[13] K. G. Klimenko, Z. Phys. C**37** (1988) 457.

[14] H. Kohyama, arXiv:0803.2109.

[15] Z. B.-Rong, Commun. Theor. Phys. **47** (2007) 520

[16] D. T. Son, Phys. Rev. D **59** (1999) 094019; T. Schafer and F. Wilczek, Phys. Lett. B **450** (1999) 325; N. J. Evans, S. D. H. Hsu and M. Schwetz, Nucl. Phys. B **551** (1999) 275.

[17] Y. Nambu, Phys. Rev. **117** (1960) 648; L. P. Gorkov, JETP **7** (1958) 993.

[18] M. L. Bellac, *Thermal Field Theory* (Cambridge University Press, 1996).